CANCER GENOMICS & PROTEOMICS 6: 149-160 (2009)

Increased Levels of Macrophage-secreted Cathepsin S during Prostate Cancer Progression in TRAMP Mice and Patients

CHARLOTTA LINDAHL[1], MONIKA SIMONSSON[1], ANDERS BERGH[1], ELIN THYSELL[2], HENRIK ANTTI[2], MALIN SUND[3] and PERNILLA WIKSTRÖM[1]

Departments of [1]Medical Biosciences, Pathology, [2]Chemistry, and [3]Perioperative Sciences, Surgery, Umeå University, Sweden

Abstract. *Background: Protein expression during prostate tumour progression in transgenic TRAMP mice was studied, with the aim of identifying proteins associated with tumour progression and castration resistant tumour growth. Materials and Methods: Protein expression was compared between normal mouse prostate, primary TRAMP tumours and peripheral metastases in long-term castrated TRAMP mice using 2-dimensional differential in-gel electrophoresis and MALDI TOF/TOF analysis. Results were verified with Western blot analysis and immunohisto-chemistry in the TRAMP model and samples from patients. Results: The active form of cathepsin S (Cat S) was identified as being significantly up-regulated in poorly differentiated TRAMP tumours and in castration-resistant metastases compared to normal mouse prostate and well-differentiated tumours. Increased Cat S levels were also found in high Gleason grade tumour areas in patients. Cat S was primarily expressed by tumour-infiltrating macrophages, as shown by double staining of Cat S and CD68 expressing cells. A significantly higher number of Cat S expressing macrophages was found in castration-resistant than in hormone naïve high grade tumours in patients. No relation was found between Cat S levels and suggested Cat S regulated, matrix-derived fragments of collagen IV or laminin 5 γ2. Conclusion: Macrophage-secreted Cat S levels increase during prostate cancer progression and could be an interesting target for therapy.*

The standard therapy for advanced prostate cancer is androgen ablation. In most patients this treatment leads to a reduction in growth of the primary tumour and probably also of metastases. Unfortunately, the effects are temporary and tumours, predominantly at metastatic sites, start to grow again despite a lack of circulating testosterone. The mechanisms behind tumour metastasis and castration-resistant tumour growth are largely unknown.

Recent studies have shown that tumour dissemination is probably an early event in prostate cancer, as well as in other forms of cancer, as dormant tumour cells can be found in up to 60% of prostate cancer patients without clinically detectable metastases, reviewed in (1). Accordingly, recurrent tumour growth is seen in about one third of patients treated with radical prostatectomy today (2, 3). Notably, tumour recurrence after therapy prostatectomy or palliative androgen-ablation therapy, is often seen at sites of distant metastasis, *e.g.* in bone, and not at the primary site. In line with this, we found that primary tumours in transgenic mice with adenocarcinoma of the mouse prostate, TRAMP (4) showed a marked response to castration, but micrometastases did not respond (5). The therapy effect was sustained for a long time in the primary tumours, while relapse at distant sites was frequently seen during the study period. Our results indicate that TRAMP cancer cells disseminate at an early stage of the disease and, furthermore, that castration therapy controls prostate cancer cells more efficiently in the prostatic milieu than at distant sites, thus similarly to what is observed in the clinic.

We have therefore used the TRAMP model and two-dimensional differential in-gel electrophoresis (2-D DIGE) technique to study protein expression during prostate tumour progression, with the aim of identifying differentially expressed proteins related to tumour progression and castration-resistant tumour growth. Protein expression was compared between normal mouse prostate, primary TRAMP tumours with different histological grade and peripheral metastases in long-term castrated TRAMP mice.

Among approximately 300 differentially expressed proteins, cathepsin S (Cat S) was identified as one protein of special interest. Cat S belongs to a family of cysteine proteases generally known as lysosomal-activated proteins which mediate bulk proteolysis (reviewed in 6). Recent

Correspondence to: Pernilla Wikström, Department of Medical Biosciences, Pathology, Umeå University, Umeå, S-90187 Sweden. Fax: +46 907852829, e-mail: pernilla.wikstrom@medbio.umu.se

Key Words: Proteomics, tumour marker, Western blot, immuno-histochemistry.

studies have however revealed many other functions for cathepsins (reviewed in 7) and there is emerging evidence that they play an important role during tumour progression by remodelling the extracellular matrix in the tumour microenvironment, thereby promoting tumour invasion and metastasis (8-10). Cat S-deficient mice show defective microvessel formation during wound healing (11) and Cat S deficiency has also been shown to impair tumour angiogenesis in the RIP1-Tag2 tumour model (12, 13). Angiogenesis-stimulating effects of Cat S could partly be caused by elimination of type IV collagen-derived angiogenesis inhibitors arresten and canstatin, and/or by enhancing the production of pro-angiogenic γ2 subunits (γ2' and γ2χ) from laminin-5 (13). High levels of Cat S have been reported in some human malignancies including glioma, astrocytoma, and lung and prostate cancer (14-17), but very little is known about Cat S expression during prostate tumourigenesis.

Materials and Methods

Animal samples. The TRAMP tumour model was developed by Dr. Greenberg and co-workers by using a region of the androgen-regulated probasin promoter to target expression of the semian virus 40 (SV 40) early-region tumour genes (T and t, Tag) to the prostate epithelium. The Tag antigens have the ability to induce transformation *in vivo*. Female C57Bl/6 TRAMP mice heterozygous for the Probasin SV-40 Tag transgene were kindly provided by Dr. Greenberg, Baylor College of medicine, Houston, TX, USA, and bred with non-transgenic C57Bl/6 males (Taconic M&B, Ry, Denmark). Tail DNA was isolated from all mice, and transgenic animals were identified *via* polymerase chain reaction (PCR) based screening, as previously described (4, 18). Transgenic mice were randomly assigned into groups and sacrificed after 17, 24 or 36 weeks.

In order to study long-term effects of castration, 24-week-old TRAMP mice were anesthetized with a cocktail containing hypnorm:dormicum:H_2O (1:1:2, 0.2 ml/30 g) and castrated *via* scrotal incision and then followed to about 52 weeks of age, or until symptoms appeared and large abdominal tumours were found at palpation. The dorsolateral and ventral lobes of the prostate (DLP and VP) and macroscopic lesions, suspected to be tumour metastases, were dissected during anaesthesia, weighed and fixed in phosphate-buffered formalin and paraffin embedded or frozen in liquid nitrogen and stored at –70˚C. For histological evaluation paraffin-embedded and frozen sections (4 μm) were routinely stained with Mayer's hematoxylin and eosin (H&E). The prostatic tissues were histologically evaluated and graded as normal, prostatic intraepithelial neoplasia, or well, moderately, or poorly differentiated adenocarcinoma, according to the grading system previously described (5, 19). Macrometastases detected after long-term castration were defined as relapsed metastases. The design of this study was approved by the Animal Ethical Committee in Umeå, Sweden.

Patient samples. Fresh radical prostatectomy samples were cut into 0.5-cm thick slices. From these slices, samples from non-malignant and tumour tissue were punched using a 0.5 cm steel cylinder. The samples were taken from 9 patients with Gleason score 7 tumours and frozen at –70˚C within 30 minutes after surgical removal of the prostate gland. The prostatectomy specimens were thereafter fixed in 4% phosphate-buffered formalin and embedded in paraffin. Tumour and morphologically benign areas were identified in 4 μm H&E-stained sections. The tumour areas were graded as Gleason grade 3 or 4 by one pathologist (A.B.). Proteins were extracted from corresponding parts of the frozen biopsies.

In the immunohistochemical studies, formalin-fixed tumour sections from patients as described above were used together with formalin-fixed tumour specimens from two series of patients treated with transurethral resection due to voiding symptoms and no earlier history of prostate cancer (20), or due to voiding symptoms at local tumour relapse after surgical castration therapy (21), respectively. Tumours were randomly selected to include 22 tumours of high grade (GS 8-10) from hormone-naïve patients and 8 tumours of high grade (GG8-10) from castration-resistant patients. Local tumour relapse was suspected on increased serum PSA levels coupled with the appearance of lower urinary tract symptoms or an increased prostate size and histologically verified as substantial tumour growth including tumour cell proliferation indices greater than those in biopsies taken shortly after castration (21).

Informed consent was obtained from all patients and the Research Ethical Committee of Umeå University Hospital approved of the study.

Sample preparation and 2-D DIGE analysis. Tissue samples from normal DLP (n=4), well (n=5) and poorly (n=4) differentiated primary TRAMP tumours and relapsed metastases (n=5) were homogenized in 200 μl of ice-cold lysis buffer (7 M urea, 2 M thiourea, 4% CHAPS and 30 mM Tris pH 8.5) using an Ultra Torrax mixer and then sonicated for 30 s. Two μl of benzonase were added and samples were centrifuged at 12,000 rpm for 10 min. The supernatants were isolated and the protein concentration was determined using a 2-D Quant kit (Amersham Biosciences, Uppsala, Sweden) according to the manufacturer's protocol. Each protein sample was labelled with 250 pmol of CyDy DIGE Flour (Cy 3 or Cy 5) per 50 μg of protein according to the manufacturer's protocol. An internal standard, a mixture of equal amounts of protein from all samples included in the experiment, was labelled with Cy 2 and included in all gels. IPG strips (24 cm, pH 3-10 NL; Bio-Rad laboratories, Hercules, CA, USA) were rehydrated with labelled samples overnight with DeStreak rehydration solution and IPG buffer to a total volume of 450 μl/strip. Fifty μg of two different samples together with 50 μg of internal standard were loaded onto each strip. First dimension (IEF) was carried out using Protean IEF cell (Bio-Rad laboratories) for a total of 70 kVh. The strips were then equilibrated in a solution containing 50 mM Tris pH 8.8, 6 M urea, 30% glycerol, 2% SDS and 1% w/v DTT for 10 min and then the same solution containing 2.5% w/v iodoacetamide instead of DTT for 10 min. Before being applied to 12 % polyacrylamide gels, strips were rinsed in running buffer (24 mM Tris base, 0.2 M glycine and 0.1 % SDS). Second dimension was performed using Ettan DALT Six System under the following conditions: 5 W/gel for 30 min and then 17 W/gel for 4-5 hours. The CyDy-labelled images were acquired on a Typhoon 9400 scanner.

The quantification of protein expression was performed using DeCyder 5.0 software. Protein spots were detected in the Cy2, Cy3 and Cy5 images for each gel with the differential in-gel analysis module and normalized spot volumes were calculated. The biological variation analysis module was used to match spot maps between

different gels and to determine differences between groups. Significantly differentiating volume ratios were identified by two independent approaches. First, univariate analysis using the DeCyder 5.0 software was performed: Student's *t*-test was used and differences with a *p*-value <0.05 together with at least 100% change between compared groups were defined as significant. Secondly, normalized volume ratios were exported and multivariate statistical evaluation was performed using orthogonal projections to latent structures discriminant analysis (OPLS-DA) (22), with the aim of separating the relapsed metastases from poorly-differentiated primary tumours. OPLS-DA separates the systematic variation in the data into predictive variation (correlated to class separation) and orthogonal variation (uncorrelated to class separation). Proteins with high loading values for predictive OPLS-DA component were considered significant for differentiating between the tumour groups.

Protein identification. Preparative gels were loaded with 500 μg of protein. After electrophoresis the gels were fixed in 10% MeOH, 7% acetic acid for one hour and stained with SYPRO Ruby overnight (400 ml/gel, Bio-Rad Laboratories). Spots of interest were excised and digested with trypsin (Promega modified trypsin) at 20 μg/ml in 50 mM ammonium bicarbonate before being extracted with 50% acetonitrile (ACN), 0.1% trifluoroacetic acid (TFA) and dried in a Speed Vac Concentrator. Protein identification was carried out at the Uppsala Biomedical Centre as outlined below.

Dried protein digest was dissolved in 5 μl of 10% ACN with 0.1% TFA, and 0.5 μl sample was mixed with 0.5 μl of a saturated solution of alpha-cyano-4-hydroxy cinnamic acid on the MALDI target. Mass spectrometry (MS) and MS/MS spectra were obtained by an Ultraflex TOF/TOF MALDI mass spectrometer (Bruker Daltonic, Germany). The instrument was calibrated with peptide Standard II (Bruker Daltonic, Germany) and each spectrum was internally calibrated with trypsin auto-digestion products. Spectra were background subtracted with signals from a blanc trypsin digestion. The MS spectra were used for searches in NCBInr database using Mascot (MatrixSciences.com) search engine.

Protein extraction and Western blot analysis. Human tissue samples were homogenized using a Micro Dismembrator (B. Braun Biotech International GmbH, Melsungen Germany) at 2000 rpm for 30 s. The samples were suspended in ice-cold lysis buffer (1% Triton® X-100, 40 mM sodium acetate, 1 mM EDTA pH 5.5) and incubated for 30 min on ice, pulse-sonicated, incubated on ice for another 30 min and centrifuged at 4˚C, 14,000 rpm for 30 min. Protein concentration in the collected supernatant was determined by using BCA Protein assay reagent Kit (Pierce Chemical Co., IL, USA).

The samples (20 μg protein) were separated by 7.5 or 12% SDS-PAGE under reducing conditions and subsequently transferred to a Hybond-P PVDF membrane (Amersham Biosciences). The membrane was blocked in 5% milk or 2% bovine serum albumin followed by primary antibody incubations: Cat S (1:500, C-19; Santa Cruz Biotechnology, Santa Cruz, CA, USA), actin (1:7000; SIGMA, Saint Louis, MO, USA), arresten (1:1,000; Mab1, Wieslab AB, Sweden), laminin-5 γ2 (1:1000, C-20, Santa Cruz Biotechnology), and laminin clone D4B5 (1:500; Chemicon International, Temecula, CA, USA) all diluted in 1% BSA/PBST, and secondary anti-mouse (Amersham Biosciences), anti-goat (Jackson Laboratory, Pierce Biotechnology, IL, USA), and anti-rabbit IgG (Amersham Biosciences) antibody incubations (dilution 1:5,000-1:50,000). Protein expression was visualized using Enhanced Chemiluminiscence Advanced or Plus (Amersham Biosciences) and quantified using ChemiDoc scanner and Quantity One 4 (Bio-Rad laboratories). The C-19 laminin-5 γ2 antibody was blocked with 1:20 (w/w) excess of blocking peptide (sc-7652P, Santa Cruz Biotechnology), overnight at 4˚C, before being used in the Western blotting experiment to investigate antibody specificity.

Immunohistochemistry. Four μm paraffin sections were de-paraffinated and rehydrated according to standard procedures before being incubated with 3% H_2O_2 in methanol for 20 min. Sections were then boiled in 1 mM EDTA, pH=8, for 1 h in 2100 Retriever (HistoLab, Frölunda, Sweden) before being incubated with the Cat S antibody overnight (diluted 1:50 with DAKO diluent, DAKO, Stockholm, Sweden) and developed with SuperPicture detection kit (Zymed laboratories, South San Fransisco, CA, USA) with diaminobenzidine (DAB) as chromogen. Staining for CD68 was performed after boiling of sections in 10 mM Tris, 1 mM EDTA (pH=9) by antibody incubation overnight (Clone KP1, DAKO, diluted 1:2,000 with DAKO diluent) and visualization using the Enhanced Alkaline Phosphatase (AP) kit and Permanent Red as chromogen (Ventana, Tucson, AZ, USA). In the double staining procedure for Cat S and CD68, Cat S was detected as above and sections were thereafter directly incubated with the CD68 antibody after washing in distilled water and then visualized as above. In the double staining procedure for Cat S and F8-40, sections were first boiled in Target 1 (DAKO) for 1 hour and blocked with protein blocking agent (DAKO) before incubated with the F8-40 antibody overnight (AbD Serotec, diluted 1:100 with DAKO diluent) and developed using Envision AP kit and Permanent Red. Thereafter, sections were boiled in 1 mM EDTA, pH=8, for 5 min in a micro oven, incubated with the Cat S antibody and visualized as described above.

The volume density (percentage) of tumour tissue (epithelium and stroma) occupied by CD68- or Cat S-positive macrophages was assessed as follows: number of graticule-crossing points overlaying positive macrophages and hits over reference space were counted using a 121-point square lattice mounted in the eyepiece of a light microscope (20). Ten randomly chosen fields were evaluated in each tumour section, at ×400 magnification.

Statistics. In Western blotting and IHC analysis experiments, groups were compared by the Mann-Whitney *U*-test and paired observation with the Wilcoxon signed rank test. Correlations between continuous variables were analyzed using the Spearman rank test. A *p*-value of less than 0.05 was considered statistically significant.

Results

2-D DIGE analysis identified increased levels of cathepsin S among many differentiating proteins during tumour progression in TRAMP mice. The 2-D DIGE analysis of normal DLP, well and poorly differentiated primary TRAMP tumours and relapsed TRAMP metastases resulted in gels where more than 2,000 different protein spots could be detected in each gel (Figure 1). Univariate analysis showed about 300 differently expressed spots according to our criteria ($p<0.05$ together with at least 100% change between compared groups) and of these 26 proteins were identified (Table I). Multivariate analysis of the 2-D data using OPLS yielded a ranking list sorted by the grade of which the

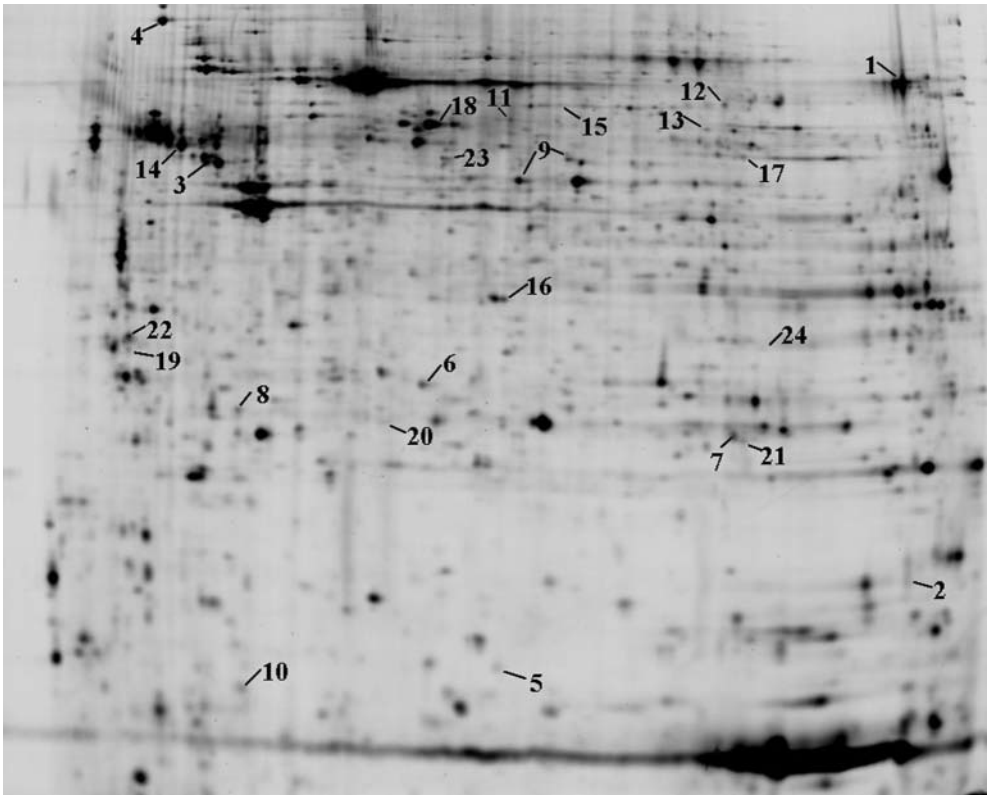

Figure 1. *Representative 2-D DIGE gel of a standard tissue sample. Fifty μg of protein extract were labelled with CyDye, multiplexed, and underwent isoelectric focusing on 24 cm pH 3-11 IPG strips. Proteins were subsequently separated on 12% polyacrylamide gels. Labeled spots were identified and numbered according to Tables I and II.*

individual spots contributed to the separation of poorly differentiated primary TRAMP tumours and relapsed metastases. We analysed the first 30 spots on the list and 13 of them were positively identified by MS/MS (Table II).

Enolase A and Cat S were found to be of primary interest as i) their levels increased from poorly differentiated primary TRAMP tumours to relapsed metastases (2.12- and 1.75-fold, respectively) and ii) they could represent important phenotypic changes of tumour cells during tumour progression regarding cell metabolism and degradation of extracellular matrix, respectively (23, 24). The enolase A protein expression was verified by Western blotting to be at higher levels in poorly differentiated tumours compared to normal tissue and well differentiated tumours, and then further increased in relapsed metastases (data not shown). Similar levels of increased enolase A has been previously shown in poorly differentiated TRAMP tumours (25). However, by using IHC, we found enolase A expression to be clearly associated with necrotic tumour areas in the TRAMP mice and in patients (results not shown) and enolase A was thereafter not further evaluated.

Cat S exists in an inactive pro-form (35-38 kDa) and in an active form (24 kDa), and on the basis of the 2-D spot localisation we concluded that it was probably the active form of Cat S that was identified as increased in the relapsed TRAMP metastases. This result was partly verified by Western blot analysis. Using an antibody which purportedly detects both the pro- and the active form of Cat S, we found significantly higher levels of active Cat S in the poorly differentiated primary tumours and in the relapsed metastases compared to normal tissue and well-differentiated tumours (Figure 2 A, C), while the level of the pro-form was unchanged (data not shown). However, the difference in Cat S expression between poorly differentiated primary tumours and relapsed metastases seen in the 2-D experiment was not detected by Western blot analysis, and the reason for this is unknown.

Western blot analysis of Cat S, arresten and laminin-5 γ2 in human prostate cancer. To evaluate if increased levels of Cat S are observed also during prostate cancer progression in patients, we used Western blot analysis to investigate levels of the active Cat S form in protein extracts from GS 7 tumours

Table I. *Differentiatinga proteins during TRAMP tumor progression identified with 2D DIGE, univariate data analysis, and MALDI-TOF/TOF.*

Spot no.	Protein name	Accession no.	Change		Mascot score	Number of peptides	Predicted mass (kDa)
			WD/N	R/PD			
1	Experimental autoimmune prostatitis antigen 1	Q8K460	–47.75	–2.13	167	18	76
2	ARMET protein	Q80ZP8	–5.42	–1.24	82	6	19
3	Protein disulfide-isomerase A6 precursor	Q922R8	–3.97	–1.03	161	13	48
4	Endoplasmin precursor	P08113	–3.35	2.72	162	23	93
5	Interleukin 25	Q9CPT4	–2.67	1.09	95	4	18
6	Endoplasmic reticulum protein ERp29 precursor	P57759	–2.65	1.36	162	23	93
7	Peroxiredoxin 6	O08709	–1.81	–1.07	137	10	25
8	Ubiquitin carboxy-terminal hydrolase L1	Q6P9V8	–1.45	–4.53	76	8	25
9	Alpha enolase	P17182	1.31	2.12	221	21	47
10	Retinol-binding protein I, cellular	Q00915	2.14	1.56	69	6	16
11	Heterogenous ribonucleoprotein A/B	Q9D6G1	2.49	1.33	75	6	30
12	Heterogenous nuclear ribonucleoprotein L	Q8R081	2.75	–1.35	109	12	61

[a]$p<0.05$ according to Student's *t*-test and with at least 100% change between compared groups; normal dorso-lateral prostate (N), well-differentiated tumors (WD), poorly differentiated tumors (PD) and relapsed peripheral metastases (R).

Table II. *Differentiatinga proteins during TRAMP tumor progression identified with 2D DIGE, multivariate data analysis, and MALDI-TOF/TOF.*

Spot no.	Protein name	Accession no.	Change		Mascot score	Number of peptides	Predicted mass (kDa)
			WD/N	R/PD			
13	Pyruvate kinase M	P52480	–1.6	–3.65	116	8	58
14	Tubulin, beta 2C	P68372	1.06	–1.95	159	18	50
15	Lamin-A/C	P48678	–1.47	–1.68	74	11	65
16	Malate dehydrogenase, cytoplasmic	P14152	1.07	–1.47	74	9	37
17	Glutathion-disulfide reductase	Q3TWI5	1.48	1.24	82	6	51
18	Protein disulfide isomeras ass prot	Q99LF6	–2.29	1.5	252	26	57
19	14-3-3 zeta	P63101	1.47	1.68	81	5	28
20	Cathepsin S	Q3UBR4	–1.16	1.75	88	6	38 / 24b
21	Ubiquinol-cytochrome *c* reductase	Q9CR68	1.13	1.76	94	6	30
22	Tropomyosin 3, gamma	P21107	1.52	1.81	114	15	33
23	Cytokeratin 8	P11679	1.29	2.78	89	13	53
24	Annexin A1	Q4FJV4	1.51	3.95	140	11	39

[a]Data were analyzed using OPLS-DA in order to find proteins that separated poorly differentiated tumors (PD) from relapsed peripheral metastases (R). N: Normal dorso-lateral prostate, WD: well differentiated tumors. [b]Predicted weight of active cathepsin S.

from 9 patients treated with radical prostatectomy. We found significantly higher levels of active Cat S in the GG4 tumour areas than in non-malignant prostate tissue areas (p=0.023, Figure 2 B, D). Active Cat S levels were also higher in GG4 than in GG3 tumour areas, with borderline significance (p=0.056, Figure 2 C, D). Arresten was abundantly expressed in all samples investigated (Figure 3), but we could not find any obvious relation between this matrix-derived angiogenesis inhibitor and active Cat S levels (data not shown). Neither did we find any association between active Cat S levels and pro-angiogenic laminin-5 γ2 subunits; an 80 kDa band (probably γ2') was detected in the prostate samples by immunoblotting that could be blocked by pre-incubation of the laminin-5 γ2 antibody with excess of peptide (C-20 antibody, Figure 4), but the intensity of this protein band did not significantly differ between groups or in relation to active Cat S levels (data not shown). Similar results were obtained when using the clone D4B5 laminin-5 γ2 antibody (results not shown).

Cat S is expressed by tumour-infiltrating macrophages and the volume density of Cat S-expressing macrophages is increased in castrated-resistant tumours in patients. We

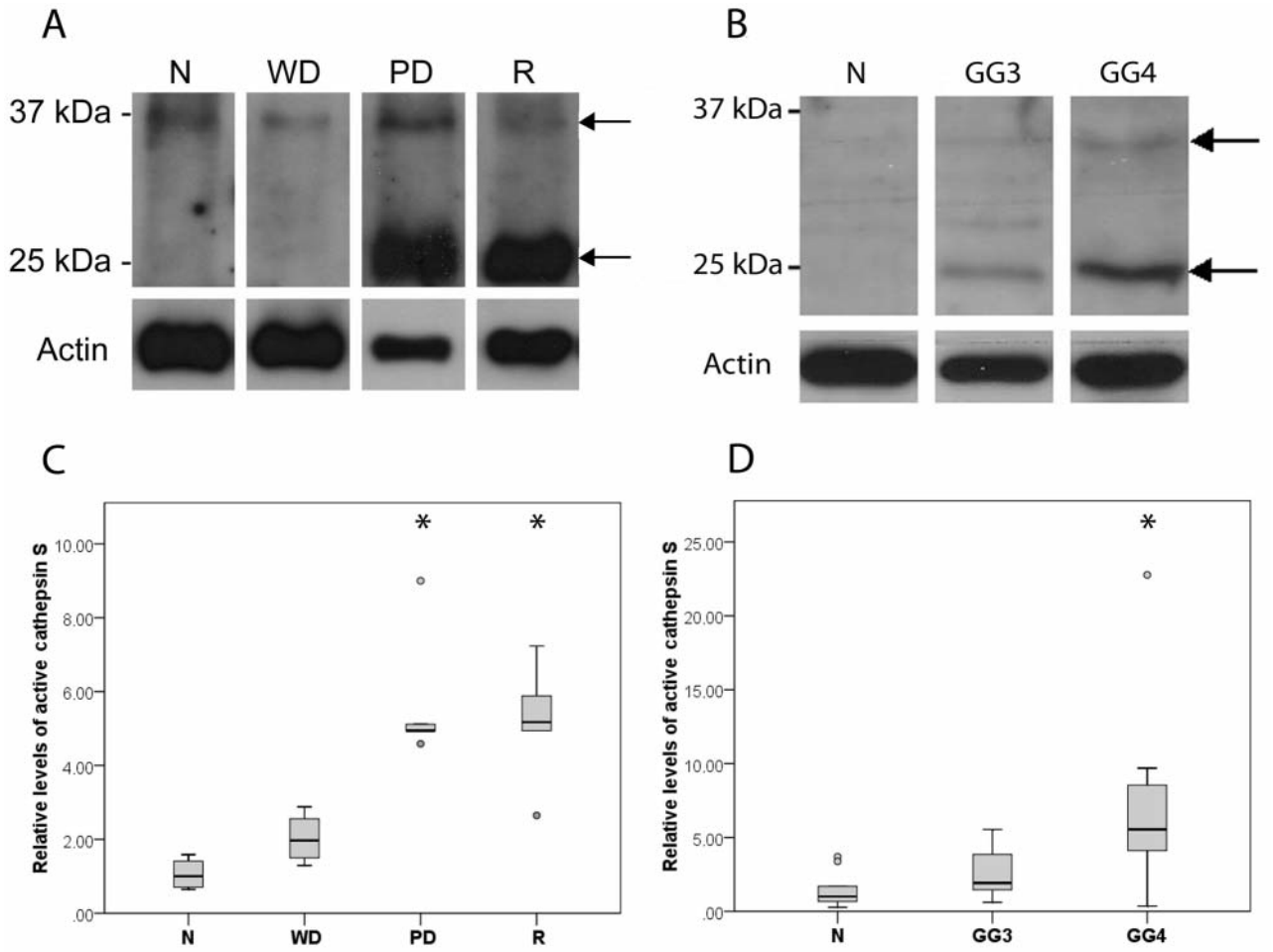

Figure 2. *Immunoblotting analysis of cathepsin S. An inactive pro-form (approximately 35 kDa) and an active form of cathepsin S (approximately 24 kDa) were detected in TRAMP mice (A) and in tumours from patients treated with radical prostatectomy (B) by Western blotting analysis (arrows). Relative levels of active cathepsin S were significantly increased in poorly differentiated (PD) primary tumours and in relapsed (R) peripheral metastases compared to well-differentiated (WD) tumours and normal dorso-lateral prostate in TRAMP mice (*p=0.023) (C). Relative levels of active cathepsin S were also increased in Gleason grade (GG) 4 tumour areas compared to normal areas (*p<0.05) and GG3 tumour areas (*p=0.056) in patients (D). n=4-9 samples per group.*

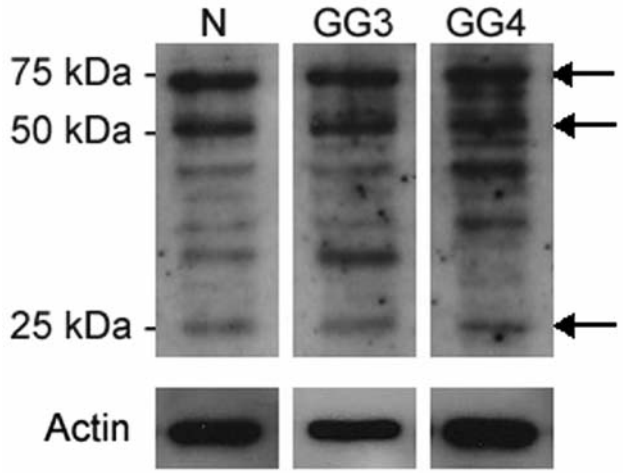

Figure 3. *Immunoblotting analysis of arresten in tumour areas from patients treated with radical prostatectomy. A 25 kDa proteolytic fragment of the type IV collagen α1-chain, arresten, was detected by Western blotting analysis. The protein bands of approximately 50 and 75 kDa are presumed to correspond to dimers and trimers, respectively, of the 25 kDa protein (arrows). N: Morphologically normal prostate; GG3 and 4: Gleason grade 3 and 4 tumour areas.*

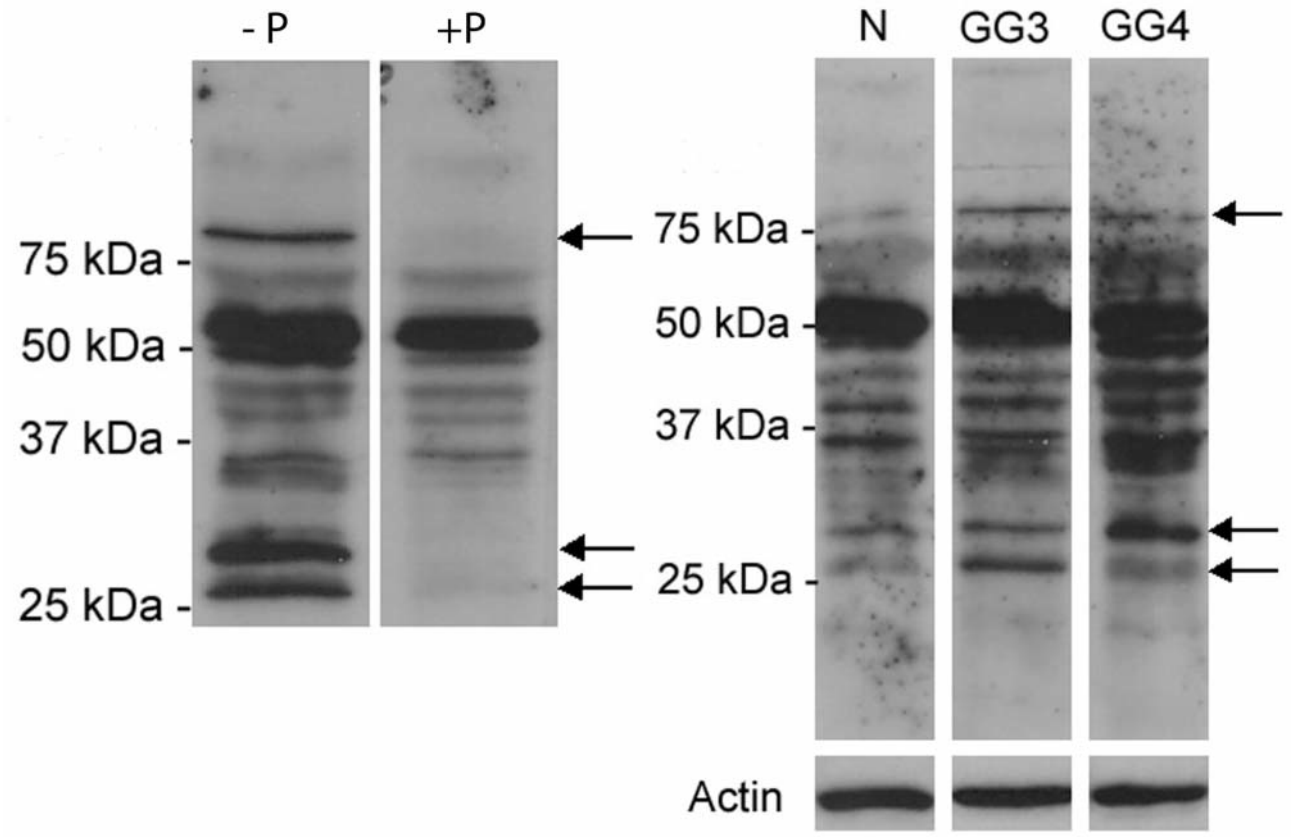

Figure 4. *Immunoblotting analysis of laminin-5 γ2 in tumour areas from patients treated with radical prostatectomy. Several protein bands were detected by Western blotting analysis. Control experiments using excess of recombinant peptide (P) specifically blocked detection of a band of approximately 80 kDa, presumed to be laminin-5 γ2', and two unknown protein bands of lower weight (arrows). N: Morphologically normal prostate; GG3 and 4: Gleason grade 3 and 4 tumour areas.*

used IHC to investigate the cellular origin of the increased Cat S levels seen in prostate tumours. Normal DLP in mice and non-malignant prostate areas in patients showed no or very few Cat S-positive cells (results not shown). Cat S-positive cells were occasionally found in well- and moderately-differentiated TRAMP tumours (Figure 5A) and in GG3 prostate tumour areas in patients (Figure 5B). High numbers of Cat S-positive cells were seen in high-grade tumours in TRAMP animals and in patients (GG4-5, Figure 5 C-F), and double staining of Cat S and F8-40 or CD68, respectively, revealed Cat S immunostaining primarily in a fraction of tumour-infiltrating macrophages (Figure 5 C-F, insets). Notably, Cat S-positive macrophages were frequently seen around vessels. Positive Cat S staining was occasionally seen also in other stroma cell types in TRAMP tumours and in castration-resistant tumours in patients (results not shown). Tumour epithelial cells remained negative in TRAMP mice and in patients (Figure 5). Interestingly, castration-resistant tumours in patients showed an increased volume density of Cat S-expressing macrophages compared to high-grade tumours in hormone-naïve patients (p=0.006), while no difference in CD68-stained macrophages was detected between those groups (Figure 6).

Discussion

In this paper we have identified increased levels of Cat S during prostate cancer progression in TRAMP mice and in patients, probably originating from a subset of tumour-infiltrating macrophages. In accordance with our results, previous studies have shown high levels of Cat S in tumour-infiltrating immune cells in a mouse model for pancreatic islet cell carcinogenesis (RIP1-Tag2) (26), and null mutation of Cat S impaired both angiogenesis and tumour growth in this tumour model (12, 13). Moreover, tumour-infiltrating macrophages have previously been associated with a poor clinical outcome in prostate cancer patients (20) and macrophage depletion has been shown to reduce angiogenesis and tumour growth in an orthotopic rat model

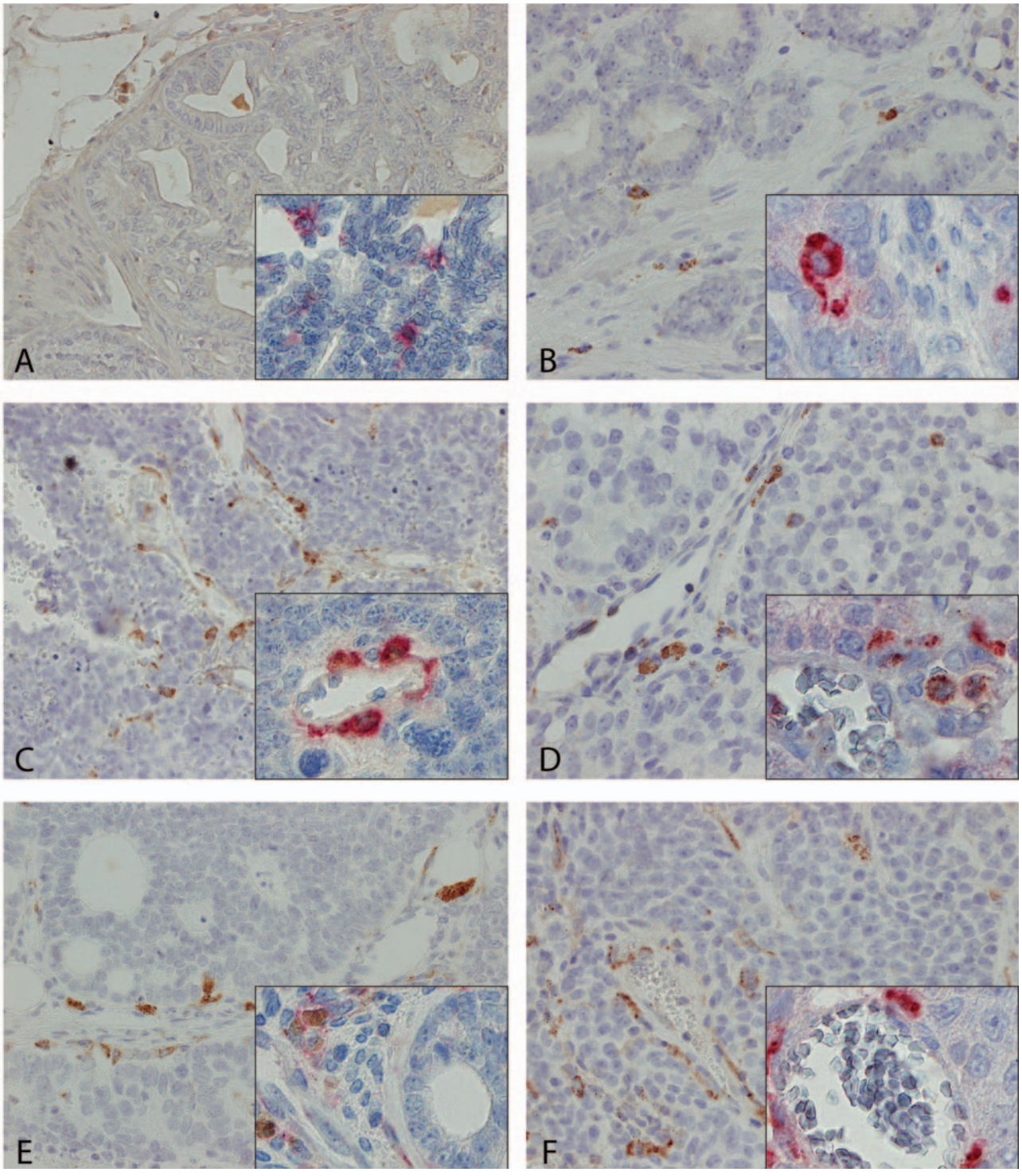

Figure 5. *Immunohistochemical staining of cathepsin S (Cat S) in TRAMP tumours (A, C, E) and in tumours areas from patients treated with radical prostatectomy (B, D) or surgical castration (F) at ×400 magnification. High numbers of Cat S-positive cells are shown in a poorly differentiated primary TRAMP tumour (C), in a GG4 tumour area from a patient treated with radical prostatectomy (D), in a relapsed kidney metastasis in a TRAMP animal treated with orchiectomy 24 weeks earlier (E), and in one castration-resistant tumour from a patient treated with surgical castration therapy 31 months earlier (F). Well-differentiated tumour areas show few Cat S-positive cells in TRAMP animals (A), as well as in patients (B). Double staining of Cat S (brown) and F8-40 (A, C, E insets) or CD68 (B, D, F insets), respectively (red), at ×800 magnification, show Cat S staining in macrophages. Note the location of Cat S positive macrophages nearby micro-vessels in high grade tumours in TRAMP mice and in patients (C-F and insets).*

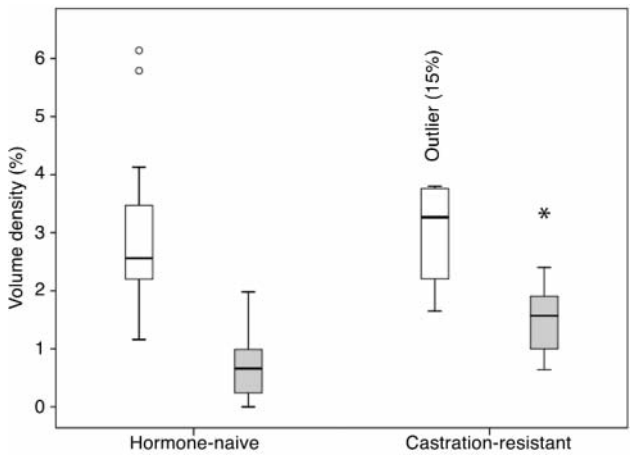

Figure 6. *Volume densities of CD68 (unfilled columns) and cathepsin S-stained (gray columns) macrophages in Gleason grade 8-10 tumours areas of hormone-naive patients (n=22) and in relapsed primary tumours of castration-resistant patients (n=8). *p=0.006 compared to hormone-naive tumours.*

of prostate cancer (27). Taken together, these results indicate that secretion of Cat S by a subset of tumour-infiltrating macrophages, often located close to tumor blood vessels, could be an important contributor to tumour growth in prostate cancer.

Cathepsin S is believed to regulate angiogenesis at least partly by proteolytic cleavage and clearance of the type IV collagen-derived anti-angiogenic fragments arresten and canstatin, as demonstrated by Wang and co-workers (13). Moreover, proteolytic cleavage of basement membrane-derived laminin 5 γ2 by Cat S into pro-angiogenic γ2' and γ2χ has been reported by the same group (13). We, however, could not find any correlation between levels of Cat S and arresten, or the γ2 subunits in this study. However, due to a lack of compatible antibodies, the potential effect of Cat S on the matrix-derived angiogenic substances was only investigated in the patient material and not in the TRAMP tumours.

According to the protein weight of Cat S detected in the 2-D and Western blot analyses, it is the active Cat S form that increases during prostate cancer progression, while the level of its pro-form does not markedly change. The inactive Cat S pro-form is normally activated in the acidic environment of lysosomes and requires an acidic environment for optimal activity (6). Prostate tumours are often hypoxic (28) and hypoxia creates an acidic milieu. Hypothetically, active Cat S could therefore be produced in fast growing, hypoxic prostate cancer areas, resulting in Cat S stimulation of tumour angiogenesis, invasiveness, and metastasis. Interestingly, Cat S is able to degrade the epithelial cell adhesion molecule E-cadherin *in vitro* (12). E-cadherin is believed to function as an invasion suppressor (29, 30) and low tumour levels of E-cadherin have been associated with metastasis and poor prognosis in prostate cancer (31). Proteolytic cleavage of E-cadherin could thereby be one way for macrophage-derived Cat S to stimulate epithelial cell invasion and migration, and, due to its perivascular location, to promote migration into blood vessels.

Increased levels of several other cathepsins: Cat B, D, H and X, have been associated with prostate cancer as well (14, 32-35) and, the ratio of Cat B to its endogenous inhibitor stefin A has been shown to predict pelvic lymph node metastasis (36). Furthermore, decreased levels of the endogenous cathepsin inhibitor cystatin C have been reported for GG 4 and 5 tumours compared to GG 2 and 3 tumours (37). We can therefore not exclude that other cathepsins could be important for prostate cancer development and progression, but still conclude that Cat S would seem to be an interesting target in prostate cancer therapy. The broad-spectrum cathepsin inhibitor JPM-OEt reduced tumour angiogenesis, invasion and growth in the RIP1-Tag2 mouse model for pancreatic cancer, at all stages of tumour development (26), and selective Cat K inhibitors have been shown to reduce bone metastasis in animal models (38). Selective Cat S inhibitors have been developed by several companies during recent years, primarily for the treatment of autoimmune conditions such as rheumatoid arthritis and psoriasis (reviewed in 39), but their anti-tumour effects have to our knowledge not yet been tested. Functional studies of anti-Cat S therapy in prostate cancer models have therefore been undertaken in our laboratory. The best effects of anti-Cat S therapy would be expected in individuals with increased tumour Cat S activity (26, 40, 41) and in combination with other therapies, such as chemotherapy, as recently demonstrated in the RIP1-Tag2 tumour model for pancreatic cancer (42).

Acknowledgements

The authors want to thank Pernilla Andersson, Elisabeth Dahlberg, Birgitta Ekblom, Sigrid Kilter and Åsa Skytt for skilful technical assistance.

Grant support: the Swedish Cancer Society, the Swedish Research Council, and the Cancer Research foundation in Northern Sweden.

References

1 Riethdorf S and Pantel K: Disseminated tumour cells in bone marrow and circulating tumour cells in blood of breast cancer patients: current state of detection and characterization. Pathobiology *75*: 140-148, 2008.

2 Amling CL, Blute ML, Bergstralh EJ, Seay TM, Slezak J and Zincke H: Long-term hazard of progression after radical prostatectomy for clinically localized prostate cancer: continued risk of biochemical failure after 5 years. J Urol *164*: 101-105, 2000.

3 Han M, Partin AW, Pound CR, Epstein JI and Walsh PC: Long-term biochemical disease-free and cancer-specific survival following anatomic radical retropubic prostatectomy. The 15-year Johns Hopkins experience. Urol Clin North Am *28*: 555-565, 2001.

4 Greenberg NM, DeMayo F, Finegold MJ, Medina D, Tilley WD, Aspinall JO, Cunha GR, Donjacour AA, Matusik RJ and Rosen JM: Prostate cancer in a transgenic mouse. Proc Natl Acad Sci USA *92*: 3439-3443, 1995.

5 Wikström P, Lindahl C and Bergh A: Characterization of the autochthonous transgenic adenocarcinoma of the mouse prostate (TRAMP) as a model to study effects of castration therapy. Prostate *62*: 148-164, 2005.

6 Turk V, Turk B and Turk D: Lysosomal cysteine proteases: facts and opportunities. EMBO J *20*: 4629-4633, 2001.

7 Vasiljeva O, Reinheckel T, Peters C, Turk D, Turk V and Turk B: Emerging roles of cysteine cathepsins in disease and their potential as drug targets. Curr Pharm *13*: 387-403, 2007.

8 Buck MR, Karustis DG, Day NA, Honn KV and Sloane BF: Degradation of extracellular-matrix proteins by human cathepsin B from normal and tumour tissues. Biochem J *282*: 273-278, 1992.

9 Mohanam S, Jasti SL, Kondraganti SR, Chandrasekar N, Lakka SS, Kin Y, Fuller GN, Yung AW, Kyritsis AP, Dinh DH, Olivero WC, Gujrati M, Ali-Osman F and Rao JS: Down-regulation of cathepsin B expression impairs the invasive and tumourigenic potential of human glioblastoma cells. Oncogene *20*: 3665-3673, 2001.

10 Mai J, Sameni M, Mikkelsen T and Sloane BF: Degradation of extracellular matrix protein tenascin-C by cathepsin B: an interaction involved in the progression of gliomas. Biol Chem *383*: 1407-1413, 2002.

11 Shi GP, Sukhova GK, Kuzuya M, Ye Q, Du J, Zhang Y, Pan JH, Lu ML, Cheng XW, Iguchi A, Perrey S, Lee AM, Chapman HA and Libby P: Deficiency of the cysteine protease cathepsin S impairs microvessel growth. Circ Res *92*: 493-500, 2003.

12 Gocheva V, Zeng W, Ke D, Klimstra D, Reinheckel T, Peters C, Hanahan D and Joyce JA: Distinct roles for cysteine cathepsin genes in multistage tumourigenesis. Genes Dev *20*: 543-556, 2006.

13 Wang B, Sun J, Kitamoto S, Yang M, Grubb A, Chapman HA, Kalluri R and Shi GP: Cathepsin S controls angiogenesis and tumour growth *via* matrix-derived angiogenic factors. J Biol Chem *281*: 6020-6029, 2006.

14 Fernandez PL, Farre X, Nadal A, Fernandez E, Peiro N, Sloane BF, Shi GP, Chapman HA, Campo E and Cardesa A: Expression of cathepsins B and S in the progression of prostate carcinoma. Int J Cancer *95*: 51-55, 2001.

15 Flannery T, Gibson D, Mirakhur M, McQuaid S, Greenan C, Trimble A, Walker B, McCormick D and Johnston PG: The clinical significance of cathepsin S expression in human astrocytomas. Am J Pathol *163*: 175-182, 2003.

16 Flannery T, McQuaid S, McGoohan C, McConnell RS, McGregor G, Mirakhur M, Hamilton P, Diamond J, Cran G, Walker B, Scott C, Martin L, Ellison D, Patel C, Nicholson C, Mendelow D, McCormick D and Johnston PG: Cathepsin S expression: An independent prognostic factor in glioblastoma tumours – a pilot study. Int J Cancer *119*: 854-860, 2006.

17 Kos J, Sekirnik A, Kopitar G, Cimerman N, Kayser K, Stremmer A, Fiehn W and Werle B: Cathepsin S in tumours, regional lymph nodes and sera of patients with lung cancer: relation to prognosis. Br J Cancer *85*: 1193-1200, 2001.

18 Greenberg NM, DeMayo FJ, Sheppard PC, Barrios R, Lebovitz R, Finegold M, Angelopoulou R, Dodd JG, Duckworth ML and Rosen JM: The rat probasin gene promoter directs hormonally and developmentally regulated expression of a heterologous gene specifically to the prostate in transgenic mice. Mol Endocrinol *8*: 230-239, 1994.

19 Kaplan-Lefko PJ, Chen TM, Ittmann MM, Barrios RJ, Ayala GE, Huss WJ, Maddison LA, Foster BA and Greenberg NM: Pathobiology of autochthonous prostate cancer in a pre-clinical transgenic mouse model. Prostate *55*: 219-237, 2003.

20 Lissbrant IF, Stattin P, Wikström P, Damber JE, Egevad L and Bergh A: Tumour associated macrophages in human prostate cancer: relation to clinicopathological variables and survival. Int J Oncol *17*: 445-451, 2000.

21 Wikström P, Ohlson N, Stattin P and Bergh A: Nuclear androgen receptors recur in the epithelial and stromal compartments of malignant and non-malignant human prostate tissue several months after castration therapy. Prostate *67*: 1277-1284, 2007.

22 Bylesjö M, Rantalainen M, Cloarec O, Nicholson JK, Holmes E and Trygg J: OPLS discriminant analysis: combining the strengths of PLS-DA and SIMCA classification. J Chemometr *20*: 341-351, 2006.

23 Altenberg B and Greulich KO: Genes of glycolysis are ubiquitously overexpressed in 24 cancer classes. Genomics *84*: 1014-1020, 2004.

24 Liuzzo JP, Petanceska SS, Moscatelli D and Devi LA: Inflammatory mediators regulate cathepsin S in macrophages and microglia: A role in attenuating heparan sulfate interactions. Mol Med *5*: 320-333, 1999.

25 Ruddat VC, Whitman S, Klein RD, Fischer SM and Holman TR: Evidence for downregulation of calcium signaling proteins in advanced mouse adenocarcinoma. Prostate *64*: 128-138, 2005.

26 Joyce JA, Baruch A, Chehade K, Meyer-Morse N, Giraudo E, Tsai FY, Greenbaum DC, Hager JH, Bogyo M and Hanahan D: Cathepsin cysteine proteases are effectors of invasive growth and angiogenesis during multistage tumourigenesis. Cancer Cell *5*: 443-453, 2004.

27 Halin S, Häggström Rudolfsson S, Van Rooijen N and Bergh A: Extratumoural macrophages promote tumour and vascular growth in an orthotopic rat prostate tumour model. Neoplasia *11*: 177-186, 2009.

28 Rudolfsson S and Bergh A: Hypoxia drives prostate tumour progression and impairs the effectiveness of therapy, but can also promote cell death and serve as a therapeutic target. Expert Opin Ther Targets *13*: 219-225, 2009.

29 Takeichi M: Cadherin cell adhesion receptors as a morphogenetic regulator. Science 251: 1451-1455, 1991.

30 Vleminckx K, Vakaet L Jr, Mareel M, Fiers W and van Roy F: Genetic manipulation of E-cadherin expression by epithelial tumour cells reveals an invasion suppressor role. Cell *66*: 107-119, 1991.

31 Umbas R, Isaacs WB, Bringuier PP, Schaafsma HE, Karthaus HF, Oosterhof GO, Debruyne FM and Schalken JA: Decreased E-cadherin expression is associated with poor prognosis in patients with prostate cancer. Cancer Res *54*: 3929-3933, 1994.

32 Miyake H, Hara I and Eto H: Serum level of cathepsin B and its density in men with prostate cancer as novel markers of disease progression. Anticancer Res *24*: 2573-2577, 2004.

33 Nagler DK, Kruger S, Kellner A, Ziomek E, Menard R, Buhtz P, Krams M, Roessner A and Kellner U: Up-regulation of cathepsin X in prostate cancer and prostatic intraepithelial neoplasia. Prostate *60*: 109-119, 2004.
34 Hara I, Miyake H, Yamanaka K, Hara S and Kamidono S: Serum cathepsin D and its density in men with prostate cancer as new predictors of disease progression. Oncol Rep *9*: 1379-1383, 2002.
35 Waghray A, Keppler D, Sloane BF, Schuger L and Chen YQ: Analysis of a truncated form of cathepsin H in human prostate tumour cells. J Biol Chem *277*: 11533-11538, 2002.
36 Sinha AA, Quast BJ, Wilson MJ, Fernandes ET, Reddy PK, Ewing SL and Gleason DF: Prediction of pelvic lymph node metastasis by the ratio of cathepsin B to stefin A in patients with prostate carcinoma. Cancer *94*: 3141-3149, 2002.
37 Jiborn T, Abrahamson M, Gadaleanu V, Lundwall A and Bjartell A: Aberrant expression of cystatin C in prostate cancer is associated with neuroendocrine differentiation. BJU Int *98*: 189-196, 2006.
38 Le Gall C, Bellahcene A, Bonnelye E, Gasser JA, Castronovo V, Green J, Zimmermann J and Clezardin P: A cathepsin K inhibitor reduces breast cancer induced osteolysis and skeletal tumour burden. Cancer Res *67*: 9894-9902, 2007.
39 Palermo C and Joyce JA: Cysteine cathepsin proteases as pharmacological targets in cancer. Trends Pharmacol Sci *29*: 22-28, 2008.
40 Grimm J, Kirsch DG, Windsor SD, Kim CF, Santiago PM, Ntziachristos V, Jacks T and Weissleder R: Use of gene expression profiling to direct *in vivo* molecular imaging of lung cancer. Proc Natl Acad Sci USA *102*: 14404-14409, 2005.
41 Blum G, von Degenfeld G, Merchant MJ, Blau HM and Bogyo M: Noninvasive optical imaging of cysteine protease activity using fluorescently quenched activity-based probes. Nat Chem Biol *3*: 668-677, 2007.
42 Bell-McGuinn KM, Garfall AL, Bogyo M, Hanahan D and Joyce JA: Inhibition of cysteine cathepsin protease activity enhances chemotherapy regimens by decreasing tumour growth and invasiveness in a mouse model of multistage cancer. Cancer Res *67*: 7378-7385, 2007.

Received April 20, 2009
Accepted April 29, 2009